An Efficient Coupled Electromechanical Solver for Studying Human Re-entrant Arrhythmias

Nathan Kirk[1], Alan P Benson[2], Matthew Hubbard[1], Christopher Goodyer[1]

[1]School of Computing, University of Leeds, United Kingdom
[2]Institute of Membrane and Systems Biology & Multidisciplinary Cardiovascular Research Centre,
University of Leeds, United Kingdom

Abstract

The study of cardiac arrhythmias is a major focus of computational biology, and undertaking biophysically detailed simulations is computationally demanding. An efficient coupled electromechanical solver to model cardiac tissue has been developed. This provides features to model fibre direction, and utilises computationally efficient techniques to reduce the simulation times. In this paper the break up of human re-entrant arrhythmias has been simulated. The results suggest that tissue deformation is a contributory factor in the break up of stable re-entrant spiral waves.

1. Introduction

The study of cardiac arrhythmias is a major topic in computational biology, as a detailed quantitative description of the underlying electrophysiology has been developed that allows the simulation of both normal and pathological excitation and the propagation of this excitation [1]. The results of such simulations can be analysed in time and space, allowing a detailed study at the cell, tissue and organ levels of the mechanisms underlying arrhythmias.

Recently, these electrophysiological models have been coupled to mechanical models in deforming domains in order to investigate the additional influence that mechanics has on arrhythmogenesis [2]. However, these are often either phenomenological models that, due to their simplicity, limit the application of the model to a disease state, or are biophysically detailed and therefore very demanding computationally.

Here we present a biophysically detailed yet efficient coupled electromechanical model of human cardiac tissue than can be used to study re-entrant arrhythmias in both healthy and diseased states.

2. Methods

To simulate cardiac electromechanical activity it is necessary to model the propagation of the electrical waves around the heart muscle, the muscle contraction instigated by this electrical activity and the feedback that the electrical activity and muscle deformation have upon each other.

2.1. Cardiac electrophysiology

A monodomain model was used to represent cardiac electrophysiology, described by the following parabolic partial differential equation [3]:

$$C_m \frac{\partial V}{\partial t} = -(I_{\text{ion}} + I_{\text{stim}}) + \nabla \cdot D\nabla V, \qquad (1)$$

where D is the diffusion tensor, C_m is the membrane capacitance, V is the transmembrane potential, I_{ion} is the sum of all ionic currents, and I_{stim} is the externally applied transmembrane current.

The ionic currents (I_{ion}) used were given by the ten Tusscher and Panfilov 2006 model [4], which provides a detailed description of the individual ionic currents, voltage and intracellular ion concentrations. This model is based on human electrophysiological data and provides the potential to simulate conditions such as end-stage tissue disease. The diffusion tensor is chosen to simulate fibre direction where the electrical currents travel faster along the fibres than across them [5].

Equation (1) is approximated using the Galerkin Finite Element Method (FEM) with linear basis functions. The simulations presented in this paper are undertaken in two dimensions and the domain is divided into unstructured triangles. The time derivative is discretised using a hybrid approach in which the Crank-Nicolson method is used for the diffusion term (for which it is unconditionally stable [6]) and an explicit forward Euler method is applied to the reaction term. The sparse system resulting from the implicit FEM approximation is solved using an ILU preconditioned GMRES solver [7].

2.2. Modelling cardiac mechanics

The cardiac tissue is modelled as a non-linearly elastic material. The stress equilibrium equation as described in [2], derived from the conservation of linear momentum following Newton's laws of motion [8], is solved to provide material deformation. In common with other authors [9, 10] the tissue is incompressible and this is enforced as described in [11]. The resulting equations are expressed as:

$$\frac{\partial}{\partial X_M} \left(T^{MN} F_N^j \right) = 0, \tag{2}$$

$$det(F) = 1, \tag{3}$$

where T^{MN} is the second Piola-Kirchhoff stress tensor and F is the deformation gradient tensor:

$$F_M^i = \frac{\partial x_i}{\partial X_M}, \tag{4}$$

where x_i are the deformed coordinates and X_M are the reference coordinates.

In common with [11], the second Piola-Kirchhoff tensor is split into an elastic component and a biochemical component, and is given by:

$$T^{MN} = \frac{1}{2} \left(\frac{\partial W}{\partial E_{MN}} + \frac{\partial W}{\partial E_{NM}} \right) - p C_{MN}^{-1} + T_a C_{MN}^{-1}, \tag{5}$$

where W is the scalar strain energy function, E the Lagrangian Green strain tensor, p (referred to as the pressure) is a Lagrange multiplier that is used to enforce the incompressibility constraint, T_a is the active tension generated by the electrical system, and C is Green's strain tensor ($C = F^T F$). The active tension is simplified as described in [11] and this ensures the force acts along the fibre direction [10, 12]. The strain energy function W from [2] is used, which describes certain types of rubbers and silicone gels, known as Mooney-Rivlin materials.

The governing equations are approximated with the FEM, using unstructured triangular elements to discretise the domain. The deformation unknowns are solved using quadratic basis functions and the pressure unknowns with linear basis functions [13]. The resulting system is highly non-linear and is solved with a matrix-free Newton-Krylov iterative method [14]. This uses a GMRES solver to solve the inner system. The non-linear nature of the system impacts on the performance of the solver and to improve this an ILU preconditioner is applied.

2.3. Coupling cardiac electrophysiology and mechanics

The electrical system generates an active tension for each node in the mesh and the mechanical system uses a subset of the nodes from the electrical system. In these simulations after ten time steps of the electrical system the active tension is passed from the electrical system to the common nodes in the mechanical system. The mechanical solve is then undertaken and a new tissue deformation is produced. The coordinates of the deformed tissue are then passed back to the common nodes in the electrical model and the more refined nodes have their deformation interpolated from these.

The biochemical component of the 2nd Piola-Kirchhoff tensor contains the active tension variable (T_a) and this is calculated using equations (22c) and (23) from [2]. (Note, the corrected version from the www.cellml.org website is used). The ODE described in equation (22c) of [2] is solved using an explicit Euler method.

2.4. Simulation settings

The simulations are run on a square domain which occupies the region of $0 < X_1, X_2 < 12$ cm. For the electrical simulations the domain is divided into 634,368 unstructured triangular elements using 318,065 nodes. This gives an approximate element edge of 0.21 cm. For the mechanical simulations a mesh of 2478 unstructured triangular elements and 5067 nodes is used. These nodes are common to the electrical mesh. To prevent spurious rotation and translation, and hence preserve uniqueness of the solution, the node closest to the centre of the domain is fixed in both directions and a neighbouring node at the same vertical height is fixed in the X_2 direction.

At time $t = 0$ ms the voltage of each node is set to -86.2 mV and a stimulus current (I_{stim}) of $52\,\mu\text{A}/\mu\text{F}$ is provided to the edge $X_1 = 0$ for $t < 1$ ms. To instigate a spiral wave, the upper half of the domain is clamped for 35 ms after $t = 165$ ms to -86.2 mV. This enables a steady state spiral wave to form, and in all simulations this is left running until $t = 5000$ ms to demonstrate spiral wave stability.

The electrical solve uses semi-implicit time discretisation which the time step (dt) to be set to 0.08 ms. The mechanical solver is not time dependent, but the iterative solver can fail to converge to a solution if the initial guess is too inaccurate. For these experiments the last two solves are used to extrapolate the initial guess and this is stable for $dt = 0.08$ ms.

The parameters for the generation of I_{ion} are defined in [4]. The diffusion tensor was set to be (in units of cm/ms):

$$\begin{pmatrix} 0.00154 & 0.0001711 \\ 0.0001711 & 0.00154 \end{pmatrix}, \tag{6}$$

which gives a wave speed of 0.68 m/s.

The upper bound of the active tension (T_a) is governed by the constant k_{T_a}, which is set to 9.58 kPa. This gen-

erates deformations that are quantitatively similar to the deformations in [11].

3. Results

3.1. Validating the electrical model

The electrical model was validated against [4]. This was done by running three sets of tests that correspond to the bottom three rows of the first column of Figure 7 of [4]. Figure 1 shows the results for dynamic restitution slopes of 1.1, 1.4 and 1.8 (as defined in Table 2 of [4]). The sim-
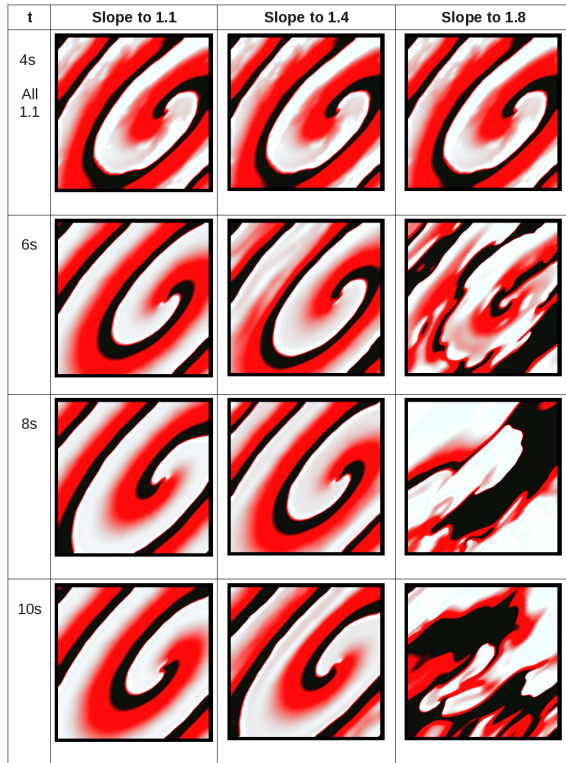

Figure 1. *Electrical model with three restitution slopes*

ulations were run for $5000\,\mathrm{ms}$ with the restitution slope set to 1.1 and then the new restitution slope introduced for a further $5000\,\mathrm{ms}$. The results in Figure 1 are similar to [4]. Specifically, for restitution slopes of 1.1 and 1.4 a stable spiral wave is maintained over time. For a restitution slope of 1.8 the spiral wave breaks up into alternans.

3.2. Validating the mechanical model

The mechanical component of the solver was validated against [11]. The left edge (where $X_1 = 0$) of the domain was fixed in space and stimulated to form a line wave. The results from this are displayed in Figure 2. These results provide deformations quantitatively similar to Figure
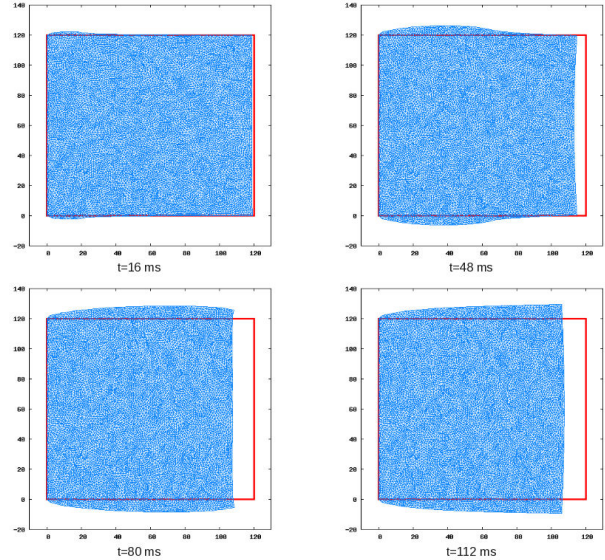

Figure 2. *Mechanical deformation caused by an electrical wave*

1 of [11] and with a similar deformation profile. It should be noted that [11] uses a different strain energy function. The tests also demonstrated a correlation between electrical wave speed and mesh resolution. On coarse electrical meshes the solution is not sufficiently resolved and this results in a wave speed dependent on the mesh.

3.3. Deforming tissue

Simulations were undertaken to compare spiral waves with the tissue deformation enabled (coupled solver) against the static domain (uncoupled solver). The results can be seen in Figure 3. In these simulations the fast sodium channel (I_{Na}) is set to the standard value as defined in [4]. The simulations were run with restitution slopes of 1.1, 1.4 and 1.8. The spiral wave is stable when the restitution slope is 1.1 for both the deforming and static simulations. The spiral wave is stable for a restitution slope of 1.4 for the static simulation and is initially stable for a restitution slope of 1.4 for the deforming simulation, however becomes unstable over time. The spiral wave for a restitution slope of 1.8 breaks up in both the static and deforming simulations.

In the deforming simulations, the domain is compressed along the fibre orientation. We can see that the deformed domain causes the spiral wave to break more quickly than in the static domain. For a restitution slope of 1.8 the wave has totally dissipated by $t = 10000\,\mathrm{ms}$ and for a restitution slope of 1.4 the wave has started to break up after $t = 8000\,\mathrm{ms}$.

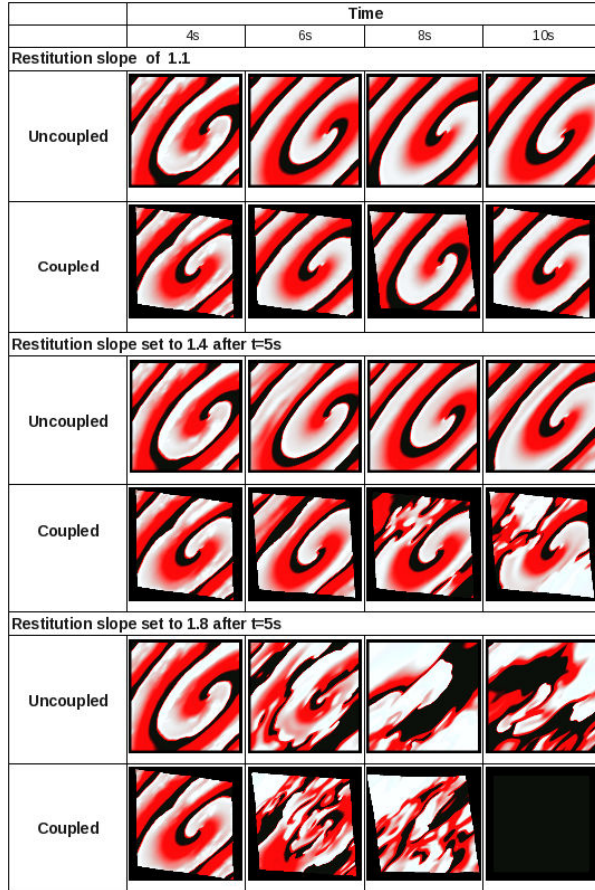|	Time			
	4s	6s	8s	10s
Restitution slope of 1.1				
Uncoupled				
Coupled				
Restitution slope set to 1.4 after t=5s				
Uncoupled				
Coupled				
Restitution slope set to 1.8 after t=5s				
Uncoupled				
Coupled				

Figure 3. *Deforming verses static domain*

4. Discussion and conclusions

A model capable of simulating cardiac tissue in a deforming two-dimensional domain has been developed. This provides the ability to model the affect of fibre direction in both the electrical and mechanical systems. The software includes a number of performance enhancement features, including using a sparse matrix storage algorithm and semi-implicit method in the electrical solver and using ILU preconditioning with re-usable numerical Jacobian in the mechanical system. We have validated this against previously published results.

In this paper the model has shown that by deforming the domain the electrical wave is altered and that this can affect the stability of a re-entrant spiral wave.

This model will now be used to simulate end-stage diseased tissue and fibrosis, introducing both in-excitable fibrotic regions and electrophysiological changes.

To fully resolve the electrical wave in these scenarios it will be necessary to add local adaptivity. This will enable fully converged solutions to be obtained using fewer mesh nodes and thus improve computational efficiency further.

References

[1] Noble D. The rise of computational biology. Nature Reviews Molecular Cell Biology 2002;3:460–43.

[2] Nash MP, Panfilov AV. Electromechanical model of excitable tissue to study reentrant cardiac arrhythmias. Progress in Biophysics Molecular Biology 2004;85:501–522.

[3] Keener J, Sneyd J. Mathematical Physiology. 1998. New York: Springer-Verlag, 1998.

[4] ten Tusscher K, Panfilov A. Alternans and spiral breakup in a human ventricular tissue model. American Journal of Physiology Heart and Circulatory Physiology 2006; 291:H1088–H1100.

[5] Jongsma HJ, Wilders R. Gap junctions in cardiovascular disease. Circulation Research 2000;86:1193–1197.

[6] Thomas JW. Numerical Partial Differential Equations: Finite Difference Methods. Texts in Applied Mathematics. New York: Springer-Verlag, 1995.

[7] Saad Y, Schultz MH. GMRES: A generalized minimal residual algorithm for solving nonsymmetric linear systems. SIAM Journal on Scientific and Statistical Computing 1986;7:856–869.

[8] Malvern LE. Introduction to the Mechanics of a Continuous Medium. Prentice-Hall, Inc, 1969.

[9] Hunter PJ, McCulloch AD, ter Keurs HE. Modelling the mechanical properties of cardiac muscle. Progress in Biophysics Molecular Biology 1998;69.

[10] Nash MP, Hunter PJ. Computational mechanics of the heart. Journal of Elasticity 2000;61:29.

[11] Pathmanathan P, Whiteley JP. A numerical method for cardiac mechanoelectric simulations. Annals of Biomedical Engineering 2009;37:860–873.

[12] Whiteley JP, Bishop MJ, Gavaghan DJ. Soft tissue modelling fo cardiac fibres for use in coupled mechano-electric simulations. Bulletin of Mathematical Biology 2007; 69:2199–2225.

[13] Gresho PM, Sani RL. Incompressible Flow and the Finite Element Method, Volume 2, Isothermal Laminar Flow. Wiley, 2000.

[14] Kelley CT. Iterative Methods for Linear and Nonlinear Equations. Society for Industrial Mathematics, 1987.

Address for correspondence:

Nathan Kirk

School of Computing, University of Leeds, United Kingdom, LS2 9JT

scnrk@leeds.ac.uk